

METALLIC NANOPARTICLE MANIPULATION USING OPTOELECTRONIC TWEEZERS

Arash Jamshidi, Hsan-Yin Hsu, Justin K. Valley, Aaron T. Ohta, Steven Neale, and Ming C. Wu
Berkeley Sensor & Actuator Center (BSAC) and Department of Electrical Engineering and Computer Sciences, University of California, Berkeley, California 94720, USA

ABSTRACT

We report on trapping of single and multiple spherical gold nanoparticles with 60 to 250 nm diameters using optoelectronic tweezers (OET). Thanks to the low optical intensities required for stable trapping (20 μW over 1.7 μm spot), we estimate the temperature increase in OET-trapped nanoparticles due to absorption to be $\Delta T < 0.1^\circ\text{C}$, making OET-trapped nanoparticles suitable for biological imaging and sensing applications. In addition, we observe translational velocities of 68 $\mu\text{m}/\text{s}$ and demonstrate trapping of both single and multiple nanoparticles in a single trap.

INTRODUCTION

In recent years, there has been much interest in metallic nanoparticles as biological nano-sensors due to their interesting optical properties [1]. However, a persistent challenge has been to find techniques for interaction with and manipulation of these nanoparticles. Optical tweezers have been used previously to trap metallic nanoparticles of different sizes [2, 3]; however, the high optical power intensities required for stable trapping ($\sim 10^7 \text{ W}/\text{cm}^2$) result in excessive heating in metallic nanoparticles ($\Delta T > 55^\circ\text{C}$) [4], hampering the application of optical tweezer-trapped particles in biological environments. Dielectrophoresis (DEP) can trap nanoparticles using fixed electrodes [5]; however, since the trapping positions are lithographically defined, fixed-electrode DEP lacks the capability to dynamically scan and manipulate the trapped particles. Trapping of single molecules has also been achieved using an Anti-Brownian Electrokinetic (ABEL) trap [6] which provides extensive information about the particle dynamics. However, this technique requires the molecules to be fluorescent.

In contrast, OET is an optical manipulation technique capable of dynamically manipulating a large number of micro and nanoparticles or cells over large areas using optical intensities 5 orders of magnitude smaller than optical tweezers [7]. Previously, the smallest particles that OET could trap were limited to nanowires of diameters below 100 nm and approximately 5 μm length [8]. In this paper, we report, for the first time, trapping of metallic spherical nanoparticles with 60 to 250 nm diameter using optoelectronic tweezers (OET).

THEORETICAL BACKGROUND

OET Device Operation Principles

Figure 1a shows the optoelectronic tweezers (OET) device structure. The OET device consists of a top and a bottom indium-tin-oxide (ITO) coated glass electrode with an AC voltage applied between the two electrodes. A 1- μm -thick layer of photoconductive material

(hydrogenated amorphous silicon) is deposited on the bottom ITO substrate. The liquid solution containing the dispersed metallic nanoparticles is sandwiched between the top ITO electrode and the photoconductor substrate. A 635-nm diode laser is used to interact with the photoconductive layer and trap the metallic nanoparticles.

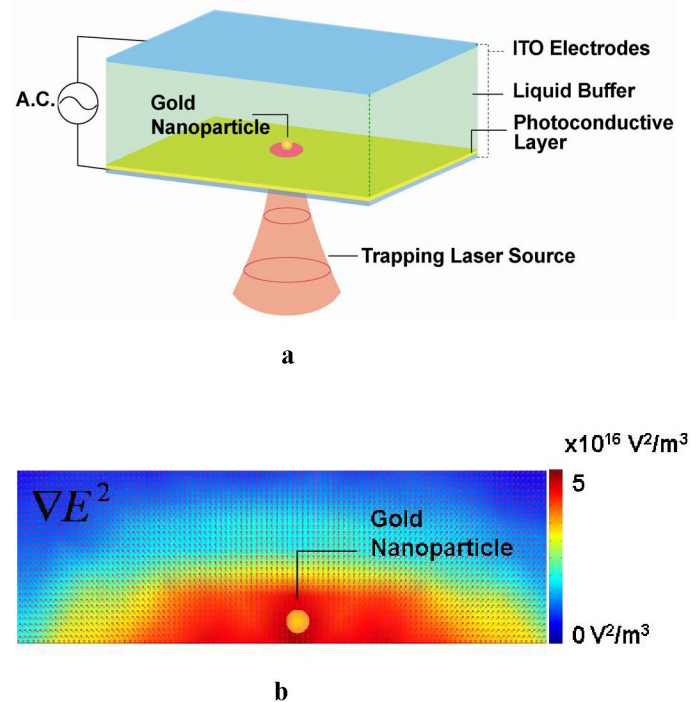


Figure 1: (a) Optoelectronic tweezers (OET) device structure for manipulation of nanoparticles. OET works based on the principle of optically-induced dielectrophoresis (DEP), where optically defined virtual electrodes create non-uniform electric fields to polarize objects in the vicinity of the fields. The objects are then attracted to or repelled from areas of high electric field intensity gradient depending on their effective induced polarization relative to the medium. The metallic nanoparticles experience an attractive (positive) DEP force due to their high polarizability relative to the liquid medium. (b) The simulated gradient of electric field intensity is shown near the OET surface. The nanoparticles are immersed and trapped in the high field gradient region near the OET surface.

When there is no laser light present, the impedance of the photoconductive layer is higher than that of the liquid layer and the majority of the applied AC voltage is dropped across the photoconductive layer. However, once the laser light is introduced, it generates electron-hole pairs in the photoconductive layer, reducing the impedance of the photoconductor layer below that of the liquid layer. Therefore, the majority of voltage is switched from the photoconductive layer to the liquid layer in the area that laser is present. Since the voltage switch occurs only in the area that laser source is present, the electric field in the liquid will have a non-uniform profile. This non-uniform field polarizes the metallic nanoparticles in its vicinity, attracting them to areas of high electric field intensity gradient according to the DEP force principle.

Figure 1b shows the finite-element simulation of the gradient of the non-uniform electric field intensity for an applied bias of 20 Vpp at 100 kHz.

Dielectrophoresis Force

The non-uniform electric field present in the liquid layer induces a dipole moment (p) in the metallic nanoparticles. The induced dipole interacts with the electric field, resulting in a dielectrophoretic force, $F = (p \cdot \nabla)E$, which attracts the nanoparticles to areas of highest field intensity gradient [9].

The DEP force expression for a spherical particle is given by [9]:

$$F_{DEP} = 2\pi r^3 \epsilon_m \text{Re}\{K\} \nabla(E^2) \quad (1)$$

where, r is the radius of the particle, ϵ_m is the permittivity of the liquid medium, $\text{Re}\{K\}$ is the real part of the Clausius-Mossotti (CM) factor given by, $\text{Re}\{K\} = \text{Re}\{(\epsilon_p^* - \epsilon_m^*) / (\epsilon_p^* + 2\epsilon_m^*)\}$, where $\epsilon^* = \epsilon - j\sigma/\omega$, with p and m subscripts referring to the particle and the liquid medium, respectively.

As shown in Figure 1b, the gradient of field intensity is strongest near the OET surface and falls off sharply as we move away from the surface. Due to the nanoparticles small size, they are immersed in the high- ∇E^2 region near the OET surface. The gradient of field intensity can be simulated using COMSOL finite-element modeling and is estimated to be $10^{16} - 10^{17} \text{ V}^2/\text{m}^3$ near the OET surface. Using this value, we can estimate the strength of the DEP force for a 100 nm diameter nanoparticle to be approximately 0.1 pN.

To estimate the velocity of the nanoparticles due to this DEP force, we can use the drag force acting on the spherical nanoparticles [10],

$$F_{Drag} = 6\pi\eta r v_{drag} \quad (2)$$

where, r is the particle's radius, η is dynamic viscosity of water, and v_{Drag} is the drag velocity. Equating this force to the DEP force ($F_{DEP} = F_{Drag}$), we can achieve v_{Drag} close to 100 $\mu\text{m/s}$.

Temperature Analysis

Using a similar analysis to ref. [4], we can estimate the temperature increase in the OET-trapped nanoparticles as $\Delta T = P_{abs} / (4\pi r C)$, where C is the thermal conductivity of water (0.6 W/K.m), r is the radial distance from the nanoparticle's center, and P_{abs} is the absorbed power in the nanoparticle given by $P_{abs} = \sigma_{abs} I^2$, where I is the laser intensity and σ_{abs} is the absorption cross section of the nanoparticle given by $\sigma_{abs} = (2\pi n_m / \lambda) \times \text{Im}[3V(\epsilon_p^* - \epsilon_m^*) / (\epsilon_p^* + 2\epsilon_m^*)]$, where $\epsilon_m^* \approx 1.77$ ($n_m \approx 1.33$) and $\epsilon_p^* \approx -10.66 + i1.37$ at $\lambda = 635 \text{ nm}$ and V is the volume of the nanoparticle. For a 20 μW trapping laser source with 1.7 μm (FWHM) spot size, we estimate the temperature increase at the surface of 60 to 250 nm diameter gold nanoparticles due to absorption to be less than 0.1°C.

It is important to note that this calculation does not take into account the temperature increase due to the joule heating in the liquid layer. The joule heating effect can be roughly estimated as [11]: $\Delta T_{joule} = \sigma_{liquid} V^2 / (2C)$, where σ_{liquid} is the liquid conductivity, V is the applied voltage, and C is the thermal conductivity of water. Using the typical experimental values for nanoparticle trapping ($\sigma_{liquid} = 1-10 \text{ mS/m}$, $V = 10-20 \text{ Vpp}$), we can estimate the temperature increase due to joule heating to be of orders of a few °C which is about an order of magnitude larger than the temperature increase due to absorption in metallic nanoparticles. Therefore, joule heating would be the dominant effect in calculating the total temperature increase in the trapping environment.

EXPERIMENTAL RESULTS

Experimental Setup

Figure 2 shows the experimental setup used for the metallic nanoparticle manipulation using OET. Gold nanoparticles with 60 to 250 nm diameters with an approximately 10^{10} particles/ml density were diluted in a 2.6 mS/m conductivity solution of DI water and KCl. 4 μL of the sample was introduced into the OET device. Majority of the nanoparticles showed strong Brownian while a portion of the particles adhered to the surface. A 635 nm diode laser with 20 μW power and 1.7 μm (FWHM) optical spot size at the OET surface was used to trap the nanoparticles. AC voltages of 10-20 Vpp at 50-100 kHz frequency were applied to the OET device. Dark field microscopy using a BX51M Olympus microscope was used to visualize the nanoparticles and images were captured using a CCD camera.

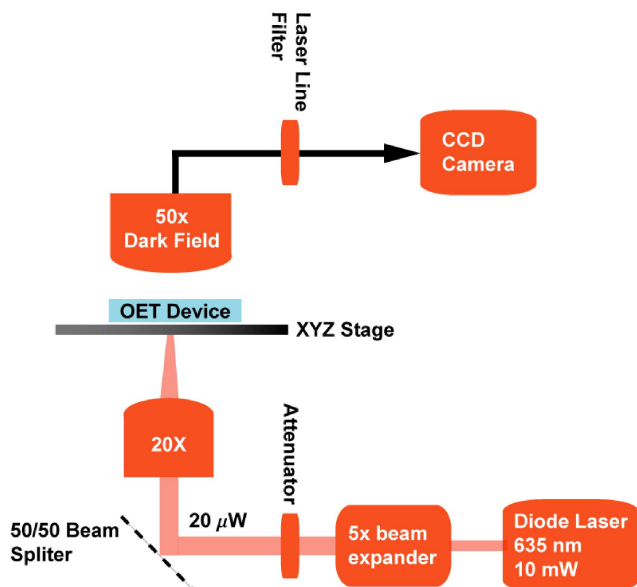


Figure 2: Experimental setup for manipulation of metallic nanoparticles. A 10-mW, 635 nm diode laser was expanded 5 \times , attenuated to 20 μ W, and focused onto the OET chip with 1.7 μ m (FWHM) using a 20 \times objective lens. The nanoparticles were visualized using dark field microscopy and a CCD camera.

DEP Manipulation of Metallic Nanoparticles

Figure 3 shows trapping of a single 100 nm gold nanoparticle using OET. The nanoparticle experiences a positive DEP force and is attracted to the laser trapping source. By manually adjusting the laser trap position, the nanoparticle is transported over an approximately 200 μ m² area in 12 seconds.

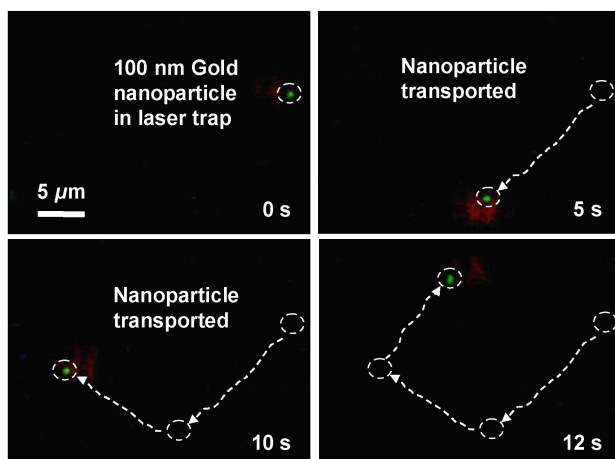


Figure 3: Trapping and transport process of a single 100 nm gold nanoparticle using OET. The nanoparticle is transported over an approximately 200 μ m² area in 12 seconds.

Trap Characterization

To quantify the maximum trapping speed of the metallic gold nanoparticles, we used an ESP-300 Newport motorized actuator controller and a LTA-HL motorized actuator to move the microscope stage relative to the optical pattern. Figure 4 shows the maximum translational speeds of 100 nm gold nanoparticles as a function of the

applied AC voltage. The experimental data follows a quadratic trend (black fitted line) which is expected since the DEP force is proportional to the gradient of the field intensity.

A 68 μ m/s maximum translation speed is measured for an applied AC voltage of 20 Vpp. This measured translational speed is close to the calculated speeds for metallic nanoparticles. In addition, a maximum trapping radius of approximately 28 μ m is measured at 20 Vpp.

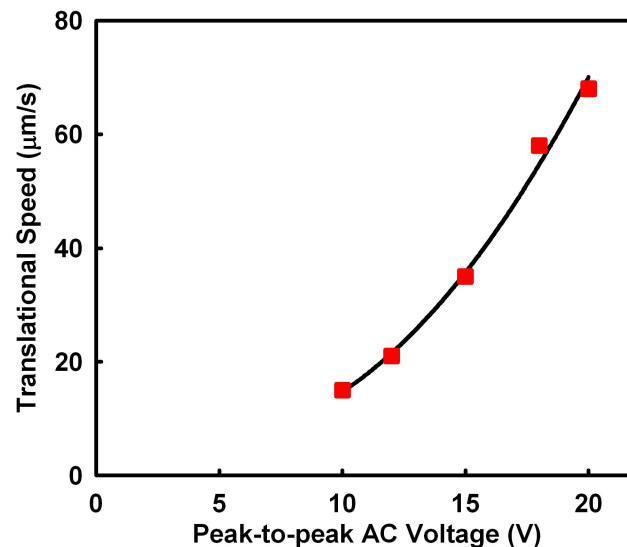


Figure 4: OET-trapped nanoparticles' translational speed as a function of the applied voltage. A maximum translational speed of 68 μ m/s at 20 Vpp is achieved. The experimental data follows a quadratic trend (black fitted curve). This is expected since the DEP force is proportional to ∇E^2 .

When more than one nanoparticle is trapped in the laser, the particles experience a mutual repulsive force due to two effects. First, nanoparticles carry a negative surface charge with a zeta potential of $\zeta = -70$ mV resulting in a mutual coulombic repulsion. Second, the dipoles induced in the nanoparticles interact with each other resulting in a dipole-dipole repulsive force which is a function of the applied voltage. By measuring the translation speeds of the particles after removing the laser trap, we can calculate the net repulsive force between two 100 nm gold nanoparticles to be approximately 23 fN at 20 Vpp (Figure 5a).

We can also observe this repulsive force acting on more than two particles as shown in Figure 5b for three nanoparticles. In the beginning the three particles are trapped in the laser source (filtered out), once the laser trap is removed, the mutual repulsion between the particles repels them from each other.

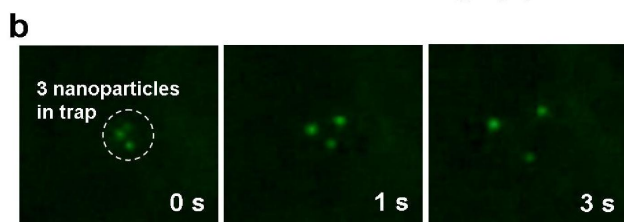
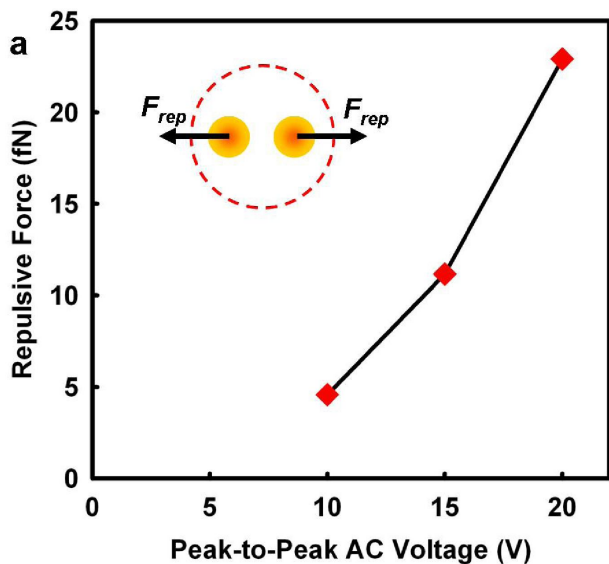


Figure 5: (a) The repulsive force (F_{rep}) between two nanoparticles (due to dipole-dipole interaction and coulombic repulsion) as a function of applied voltage. (b) The repulsive force interaction is also observed for three nanoparticles. In the beginning, the particles are trapped using OET (laser filtered out), once the trap is removed, the nanoparticles repel each other.

Trapping of Multiple Nanoparticles

Figure 6a-d shows trapping and transport of five 250 nm gold nanoparticles using OET. Nanoparticles are concentrated in the OET trap and can be transported by scanning the laser trap manually, once the laser trap is removed, nanoparticles undergo Brownian motion and the five gold nanoparticles are distinctly observable. The ability to concentrate the nanoparticles in a single spot is important to enhance the sensitivity of the dynamic hot-spots for imaging and sensing applications.

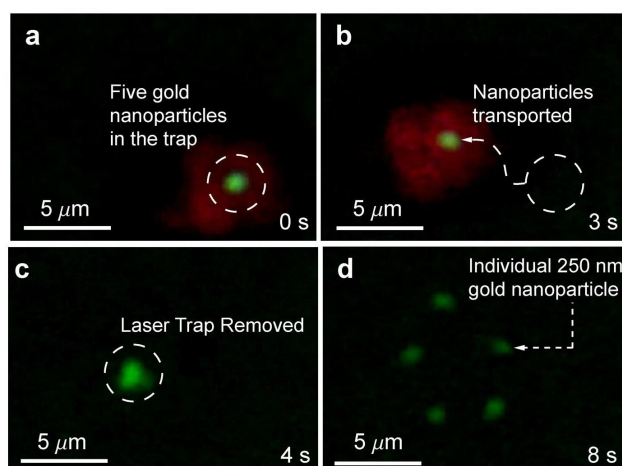


Figure 6: Trapping and transport of five 250 nm gold nanoparticles. (a) Nanoparticles are trapped and

concentrated in the laser trap. (b) Nanoparticles are transported to a new location by manually adjusting the laser position. (c) Laser trap is removed and nanoparticles undergo Brownian motion. (d) Five gold nanoparticles are distinctly observable after removal of the trap.

CONCLUSION

In conclusion, we report on trapping single and multiple spherical gold nanoparticles with 60 to 250 nm diameters using optoelectronic tweezers. Due to low optical intensities required for stable trapping we estimate the temperature increase in OET-trapped nanoparticles due to absorption to be $\Delta T < 0.1^\circ\text{C}$. In addition, we observe translation speeds of $68 \mu\text{m/s}$ for 100 nm gold nanoparticles at 20 Vpp applied voltage.

ACKNOWLEDGEMENT

This work was supported in part by the National Institutes of Health through the NIH Roadmap for Medical Research (Grant #PN2 EY018228) and DARPA. We also thank Lawrence Berkeley National Laboratory (LBNL) Molecular Foundry and UC Berkeley Microfabrication Laboratory.

REFERENCES

- [1] Anker, J.N., et al., *Nature Materials* 7, pp. 442 - 453 (2008).
- [2] Svoboda, K. and Block, S. M. *Optics Letters* 19, pp. 930 - 932, (1994).
- [3] Hansen, P. M., et al., *Nano Letters* 5, pp. 2429 - 2431, (2005).
- [4] Seol, Y., Carpenter, A. E., Perkins, T. T., *Opt. Lett.* 31, pp. 1937 - 1942, (2006).
- [5] Zheng, L., Li, S., Brody, J. P., Burke, P. J., *Langmuir* 20, pp. 8612-8619, (2004).
- [6] Cohen, A. E., Moerner, W. E., *Optics Express* 10, pp. 6941-6956, (2008).
- [7] Chiou, P.Y., Ohta, A. T., Wu, M. C., *Nature*, 436, pp. 370-372, (2005).
- [8] Jamshidi, A., et al., *Nature Photonics* 2, pp. 85 - 89, (2008).
- [9] T. B. Jones, *Electromechanics of Particles* (Cambridge: Cambridge University Press), 1995.
- [10] H. Morgan and N. Green, *AC Electrokinetics: colloids and nanoparticles* (Research Studies Press Ltd.), 2003.
- [11] Ramos, A., et al., *J. Phys. D: Appl. Phys.* 31, pp. 2338 - 2353 (1998).